Journal of Applied Polymer Science

The unique morphology role of thorn surface in determining electrochemical performance of polyaniline nano-fibers via one-step method

Hai-yan Wang,[1] Lan Li,[2] Long Zhang,[1] Fen Ran[1]

[1]State Key Laboratory of Gansu Advanced Nonferrous Metal Materials, Lanzhou University of Technology, Lanzhou 730050, China

[2]Lanzhou University of Technology, School of Petrochemical Engineering, Lanzhou 730050, China

Correspondence to: H.-y. Wang (E-mail: wanghy03@163.com) and F. Ran (E-mail: ranfen@163.com)

ABSTRACT: Polyaniline nano-fibers with thorn surface morphology (T-PANI) were synthesized by one-step polymerization with adding additional aniline at later stage of chemical oxidation synthesis. In order to investigate the morphology role in determining electrochemical performance, the nano-fibers PANI without thorn (PANI) was synthesized by the same polymerization process but at different time to add additional aniline. Material structures were characterized by field emission scanning electron microscope and Brunauer-Emmett-Teller method, and electrochemical performance was tested through cyclic voltammograms, galvanostatic charge-discharge and electrochemical impedance spectroscopy. The data showed that the specific capacitance of T-PANI was 443 F g^{-1} at 5 mA cm^{-2}, which was much more than that of PANI (338 F g^{-1} at 5 mA cm^{-2}). The solution resistance, charge transfer resistance, and diffuse resistance of T-PANI were also lower than these of PANI. The results indicate that the thorn surface structure plays an important role in determining the electrochemical performance of polyaniline, which attribute to the improvements in pore size, pore distribution, special surface area, and conductivity. © 2015 Wiley Periodicals, Inc. J. Appl. Polym. Sci. **2015**, *132*, 42266.

KEYWORDS: batteries and fuel cells; conducting polymers; electrochemistry; nanostructured polymers

Received 27 November 2014; accepted 25 March 2015

DOI: 10.1002/app.42266

INTRODUCTION

Electrochemical supercapacitors, which have been used for pulse power application, are a kind of energy-storage devices between conventional capacitors and batteries.[1] Electrochemical properties of electrically conducting polymers (ECPs), including polyaniline (PANI),[2,3] polypyrrole,[4,5] polythiophene[6] and their derivatives, represent promising electrode materials for the application of supercapacitors. It should be noted that PANI as a supercapacitor electrode materials has received universal interest in recent 20 years owing to controllable morphology, tunable properties, relative ease of synthesis and low cost.[7–9] In particular, more attention has been paid to one-dimensional PANI, such as nanofibres,[10] micro-rods,[11] nanowires,[12] and nanotubes,[9] because they are more prominent in the large surface area and porous structure.

Pore structure and special surface area have crucial impacts on ionic diffusion path. Specifically good electrolyte accessibility and facile ionic transport can lead to greatly improving special capacitance of electrode materials.[13] In recent few 10 years, researchers have made one-dimensional PANI in order to get excellent electrode materials. Interconnected fuzzy nanofibrous network of PANI electrode having diameter typically between 120 and 125 nm was electrosynthesized by Dhawale *et al.* The specific capacitance of 839 F g^{-1} was achieved at the voltage scan rate of 10 mV s^{-1} in H_2SO_4 electrolyte.[14] PANI microtubes, the length of which was 2∼3 μm and the outer diameter of which was 300∼400 nm, were prepared at low temperature with camphorsulfonic acid (CSA) as the dopant by Lü *et al.* The specific capacitance reached up to 522 F g^{-1} at 5 mA cm^{-2} in 0.2 mol L^{-1} HCl electrolyte.[15] Although many experiments on modifying one-dimensional PANI have been reported,[9,12,14,15] its surface morphology control are not paid attention to for ideal supercapacitors electrode materials.

In this work, specific capacitance of one-dimensional PANI was improved by modifying surface morphology. The method can regulate the special surface area and outer porous structure of interconnected fibers network. The role of PANI surface morphology was investigated in determining supercapacitor electrochemical performance by synthesizing PANI nano-fibers with

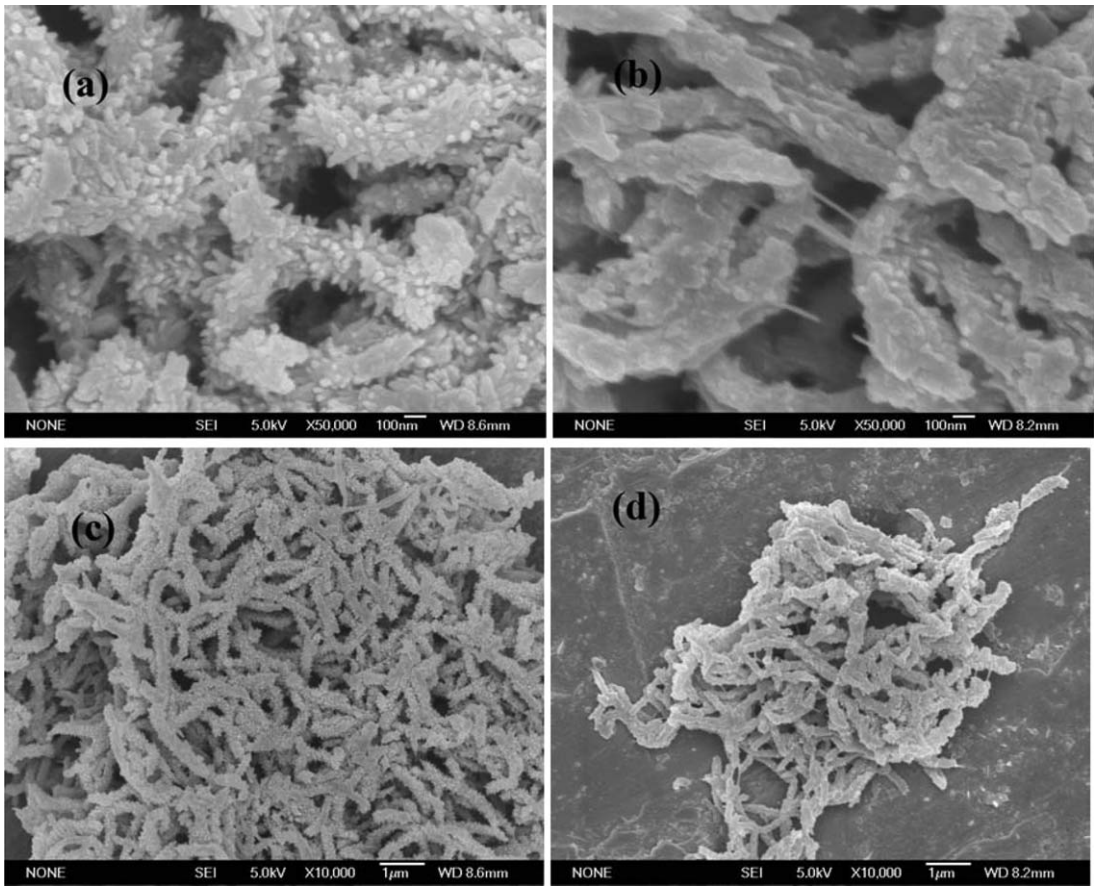

Figure 1. SEM images of T-PANI (a,c) and PANI (b,d).

thorn surface. In comparison, the PANI fibers without thorn were also synthesized.

EXPERIMENTAL

Materials

Aniline (AN, analytical purity) was purified through distillation under reduced pressure before use. Ammonium persulfate ($(NH_4)_2S_2O_8$, APS), perchloric acid and other reagents were analytical purity and used as received without further treatment. All the solutions were prepared using deionized water.

Synthesis

The polymerization of T-PANI was shown as follows: 5 mL aniline was dissolved in 100 mL perchloric acid solution. After that, 70 mL perchloric acid solution containing APS was dropwise added into the above mixture. During the reaction process, additional 0.5 mL aniline was added to the reaction solutions after 7.5 h. After filtering process, the products were washed with deionized water and ethanol until the filtrate became colorless, and then dried in vacuum condition at 40°C.

The polymerization of PANI was shown as follows: 5 mL aniline was dissolved in 100 mL perchloric acid solution. After that, 70 mL perchloric acid solution containing APS was dropwise added into the above mixture. During the reaction process, additional 0.5 mL aniline was added to the reaction solutions after 8.5 h. After filtering process, the products were washed with deionized water and ethanol until the filtrate became colorless, and then dried in vacuum condition at 40°C.

In this experiment, the reactions were allowed to proceed under agitation for 12 h at 13∼15°C. The perchloric acid solution was 1.5 mol L^{-1}, and the mole ration of aniline to APS was 2. Based on the different surface morphology, the samples were named as T-PANI (with thorn surface morphology) and PANI (without thorn), respectively.

Characterization

Morphologies of the as-prepared PANI were investigated with a 6700F field emission scanning electron microscope (JEOL Japan). Pore structure was characterized by physical adsorption of N_2 at 77 K (ASAP 2010 Micromeritics). The specific surface area (SSA) was obtained by the Brunauer-Emmett-Teller (BET) method. The micropore volume and micropore surface area were obtained using the t-plot method. The pore size distribution was calculated by the Barrett-Joyner-Halenda (BJH) method. The conductivity was measured using TH2818 Automatic Component Analyzer at ambient temperature employing the two-probe method on a pressed pellet according to the formula: $\sigma = L/RS$. Here σ, L, R, and S refer to electrical conductivity, thickness, resistance and touching area of the sample, respectively. The pellets were obtained by subjecting the powder sample to a pressure of 10 MPa. The reproducibility of the result was checked by measuring the resistance for three times for each pellet.

Figure 2. Synthesis diagram of T-PANI. [Color figure can be viewed in the online issue, which is available at wileyonlinelibrary.com.]

Electrode Preparation and Electrochemical Measurements

The working electrodes (8 mg) were prepared as follows: 80 wt % of PANI was mixed with 7.5 wt % of acetylene black and 7.5 wt % of conducting graphite in an agate mortar until a homogeneous black powder was obtained. To this mixture, 5 wt % of poly (tetrafluoroethylene) was added together with a few drops of ethanol. The resulted paste was pressed at 10 MPa into stainless steel current collector (ChangSha Lyrun New Material, 90 PPI, 2 mm), then dried at 80°C for 12 h. Each electrode contains ~8 mg of electroactive material and has a geometric surface area about 1 cm^2.

A typical three-electrode glass cell equipped with a working electrode, a platinum foil counter electrode, and a saturated calomel reference electrode (SCE) was used for electrochemical measurements of the as-prepared working electrodes. All electrochemical measurements were performed using an electrochemical working station (CHI660C, Shanghai, China) in 1*M* H_2SO_4 aqueous solution at 25°C. The corresponding specific capacitance was calculated from the following eq. (1):

$$C_m = \frac{C}{m} = \frac{I \times \Delta t}{m \times \Delta V} \quad (1)$$

where C_m (F g^{-1}) is the specific capacitance, I (A) is discharge current, Δt (s) is the discharge time, ΔV (V) represents the potential drop during discharge process, and m (g) is the mass of the active material.[16,17]

RESULTS AND DISCUSSION

Morphology

SEM images of PANI with different surface morphology were shown in Figure 1. Although similar fibers diameters (~120 nm) were observed, there was obvious different in the surface morphology of PANI and T-PANI. For T-PANI, a large quantity of uniform nano-thorns was found on PANI fibers [Figure 1(a,c)]. The diameter of the thorns lied in the range of 30~50 nm, and the length lied in the range of 40~100 nm. For PANI, there was little thorn on PANI fibers [Figure 1(b,d)]. In comparison, the hierarchical structure was found in T-PANI.

The synthesis diagram of PANI fibers with thorn surface was shown in Figure 2. Some studies suggested that the terminal aniline units become active even after the polymerization and stimulate additional chain growth after the addition of new monomer and oxidant in the termination phase.[18] In this experiment, PANI fibers were synthesized in dilute polymerization solution without the aid of specific templates, where the nucleation growth was in the effective control.[19] When the additional aniline was added into the reaction system after 7.5 h, the protuberance arrays grew on PANI fibers. When the additional aniline was added into after 8.5 h, the concentration of the oxidant was too low to go on with chain propagation. The results show clearly that PANI thorn is derived from secondary growth on the primary fibers as shown in Figure 2.

Surface Areas and Pore Structure

The two profiles in Figure 3 of both isotherms and pore size distribution were similar, indicating the similar fibrous construction characteristic. The pore size distributions of T-PANI [Figure 3(a), inset] and PANI [Figure 3(b), inset] calculated by BJH method were also similar, which agree to well with the SEM observation. But for T-PANI, the pore size centralized in less than 20 nm, and the relevant pore volume was obviously much larger than that of PANI. The adsorption average pore diameters were 113 nm (of T-PANI) and 173 nm (of PANI), respectively. The total specific surface area and pore volume of the T-PANI were also much more than these of PANI in the Table I. The gap values were 10.4 m^2 g^{-1} and 0.02 cm^3 g^{-1}, respectively. The results could be attributed to the thorn characteristic on PANI fibers. Because of the improvements in pore size, pore distribution and special surface area, the counter ions can more easily penetrate the inner layer of PANI and reach the surface and inner of the PANI fibers, realizing the efficient

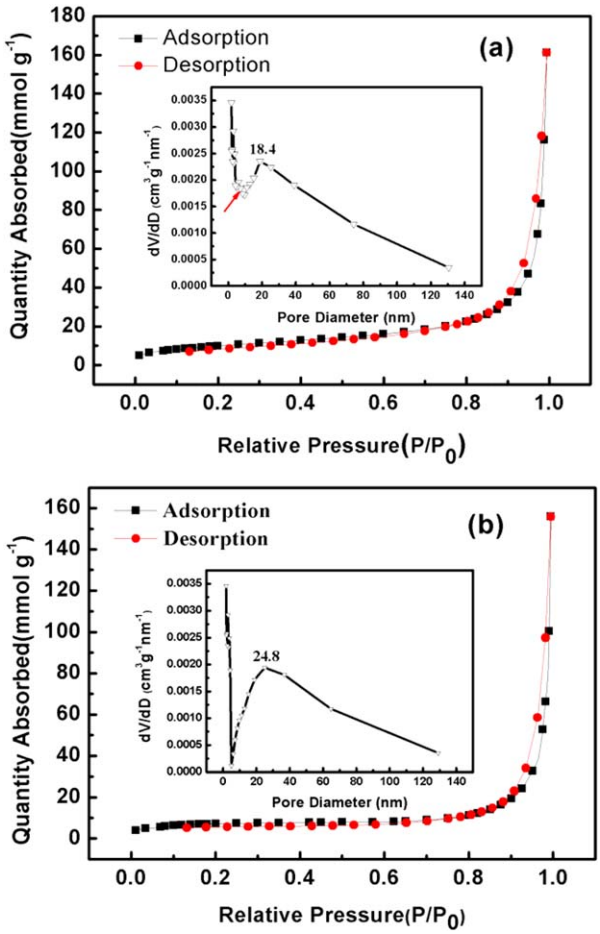

Figure 3. N_2 adsorption and desorption isotherms and pore size distribution (inset) for T-PANI (a) and PANI. [Color figure can be viewed in the online issue, which is available at wileyonlinelibrary.com.]

Table I. Specific Surface Area, Pore Volumes and Conductivity of T-PANI and PANI

Samples	BET surface area (m^2 g^{-1})	Pore volume (cm^3 g^{-1})	Conductivity (S cm^{-1})
T-PANI	36.73	0.25	3.23
PANI	26.31	0.23	2.17

utilization of the electrode materials.[20–22] In addition, the conductivity of T-PANI was 1.06 S cm^{-1} more than that of PANI in the Table I. It indicated that electrode material of T-PANI possess the better ability to transfer electronic conductivity.[23]

Electrochemical Performance

Figure 4(a) exhibits the cyclic voltammograms (CV) curves of the prepared electrode materials at a sweep rate of 5 mV $s^{-1}$and a potential range of −0.2 to 0.8 V in 1*M* H_2SO_4 solution. Both electrode materials showed two couples of redox peaks in the CV curve, in which a pair of redox peaks (A/A′) was attributed to the redox transition of PANI from leucoemeraldine (semiconducting state) to the polaronic. Emeraldine form (conducting sate) and peaks (B/B′) were due to the transformation from emeraldine to pernigraniline.[24] It could be seen that T-PANI fibers had considerably higher redox currents than PANI, and the gap value is about 0.02 A. It implied that more effective surface areas of T-PANI are accessible to the electrolytes.[20,25]

Figure 4(b) represents the typical galvanostatic charge-discharge (GCD) curves of PANI at 5 mA cm^{-2} between −0.2 and 0.8 V. As clearly seen, the charge time of T-PANI was less than that of PANI (The times were 951 and 1548 s, respectively), and the discharge time was longer than that of PANI (the gap value was 168 s). It is expected that the materials be used as an electrode material for surpercapacitors device. The initial specific capacitance value for T-PANI was 443 F g^{-1} at 5 mA cm^{-2}, which is a bit lower than that of Lü's work (522 F g^{-1} at 5 mA cm^{-2})[15], but considerably higher than that of PANI (338 F g^{-1} at 5 mA cm^{-2}). The numeral means the increase by 30% in the special capacitance due to transforming surface morphology from PANI to T-PANI. The data illustrated that T-PANI exhibit better charge-discharge properties than PANI.

The specific capacitance of T-PANI and PANI were tested at range from 5 to 50 mA cm^{-2}. The obtained capacitance values were used to calculate the energy density (*E*) and the power density (*P*). Based on the following equations,[26] the curves of *E* and *P* for the two samples were given in Figure 6(c).

$$E = \frac{1}{2} C_m \Delta V^2 \tag{2}$$

$$P = \frac{E}{\Delta t} \tag{3}$$

It was observed that the energy density of two samples dropped off with the increase of power density. But the energy density of T-PANI still remained higher than that of PANI, implying that T-PANI shows excellent electrochemical performance as supercapacitor's material.

EIS gives the important information about conductivity studies and elucidating the mechanism and kinetics of the chemical and electrochemical reactions on PANI electrodes.[27–29] Figure 5 represents equivalent circuit (a), bode curves (b), and Nyquist impedance plots (c) of T-PANI and PANI. Each of

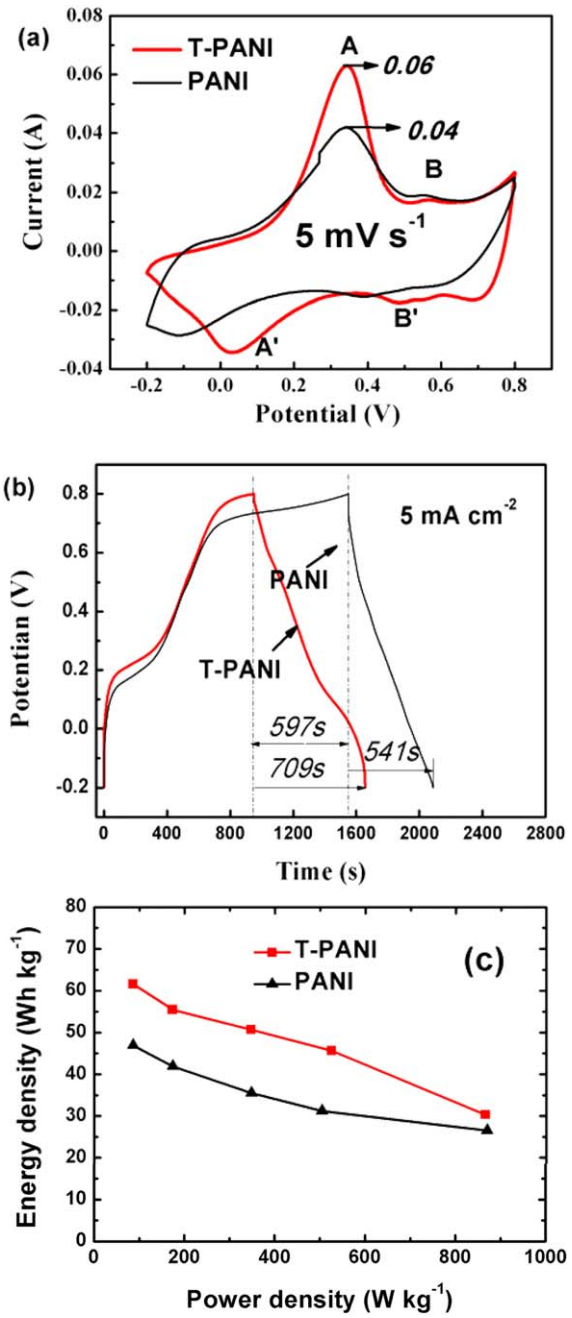

Figure 4. (a) Cyclic voltammograms at a scan rate of 5 mV s^{-1}, (b) initial charge-discharge behaviors at a current density of 5 mA cm^{-2}, and (c) plots of specific energy density vs. specific power density. [Color figure can be viewed in the online issue, which is available at wileyonlinelibrary.com.]

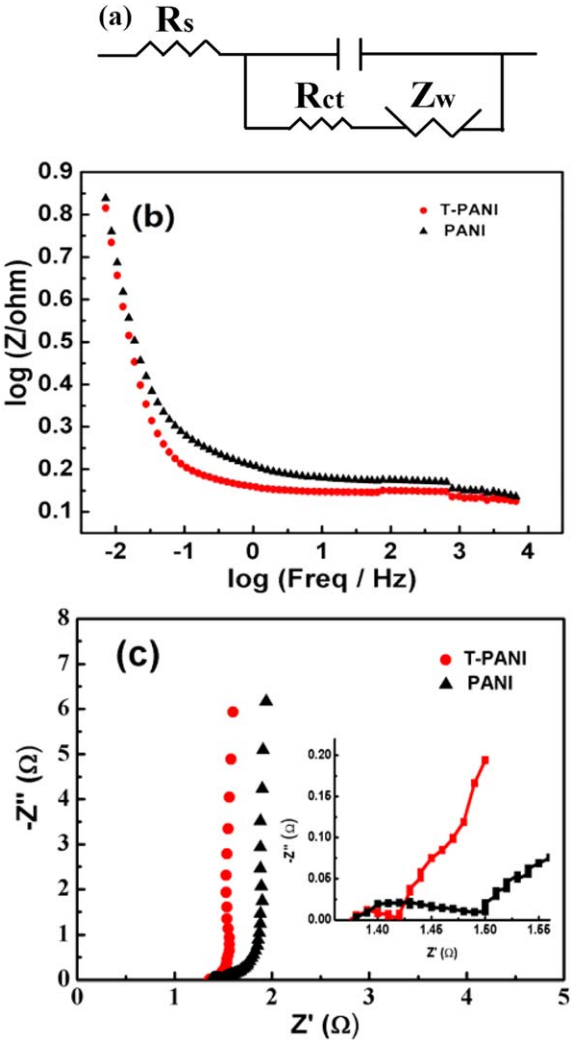

Figure 5. Equivalent circuit, Bode curves and Nyquist impedance plots of T-PANI and PANI. [Color figure can be viewed in the online issue, which is available at wileyonlinelibrary.com.]

the curves in Figure 5(c) consists of a distorted semicircle in the high frequency (HF) region and a straight line in the low frequency (LF) region. In HF region, the intersection of the plots at the x-axis represents the R_s, which is equal to the solution resistance.[30] The diameter of the semicircle is equal to the electrode resistance, which arises from the charge transfer resistance (R_{ct}). The data are shown in Table II. The R_{ct} and R_s values of T-PANI were 0.03 and 0.02 less than these of PANI, respectively. The low R_s and R_{ct} values from T-PANI are beneficial for the fast transportation of ions and electrons, consistent with the good reversible electrochemical activity obtained by CV tests in Figure 4(a) and high conductivity in Table I. In LF region, the line represented the diffusive resistance (Warburg impedance) of the electrolyte ions diffusion in host materials. Each vertical spectrum exhibited the domination of the capacitive behavior at the electrolyte and sample interface.[31] Interestingly, the Warburg impedance of T-PANI electrode was also lower, which was attributable to more effective transfer electronic ability owing to good porous structure.

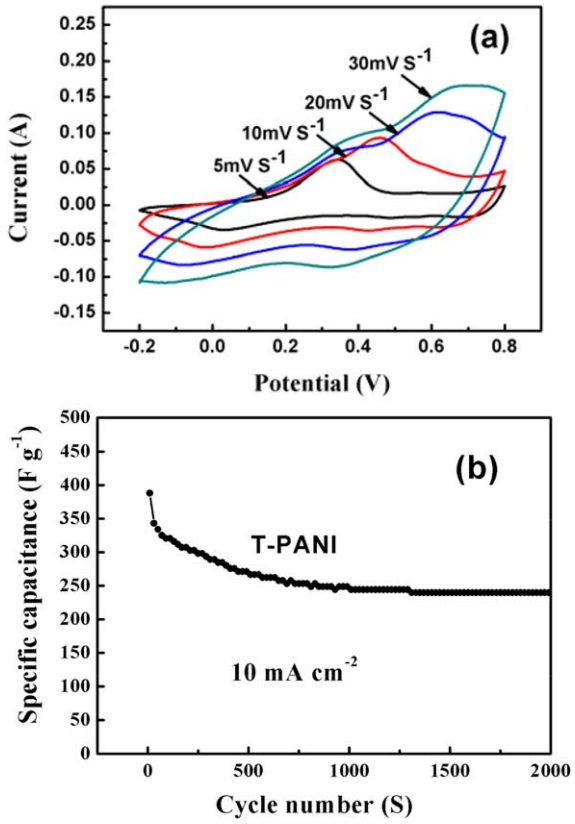

Figure 6. (a) Cyclic voltammograms of T-PANI at different sweep rates and (b) change trend of capacitance of T-PANI as the cycle number is increased at a current density of 10 mA cm^{-2}. [Color figure can be viewed in the online issue, which is available at wileyonlinelibrary.com.]

These results were consistent with their specific capacitance values in Table II.

As a representative system, the CV curves of T-PANI at various scan rates are shown in Figure 6(a). All of CV curves showed two pairs of redox peaks, indicating that the electrode is stable in acid electrolyte within the applied potential window. In order to further understand the electrochemical stability of T-PANI electrode, consecutive charge-discharge cycles were measured at a current density of 10 mA cm^{-2}. As shown in Figure 6(b), the specific capacitance values decreased gradually during 1000 charge-discharge cycles, and finally remained stable at about 250 F g^{-1} that was about 30% of its initial capacitance. After 1000 cycles, the capacitance values remain stable.

CONCLUSION

Nano-fiber PANI with thorn surface morphology was synthesized by adding additional aniline at the later stage of chemical

Table II. Impedance Parameter Values from the Fit to the Equivalent Circuit for Impedance Spectra and the Specific Capacitance of T-PANI and PANI

Sample	R_{ct} (Ω)	R_s (Ω)	C_m (F g^{-1})
T-PANI	0.09	1.35	443
PANI	0.12	1.37	338

oxidation synthesis. The electrochemical performance of such a T-PANI was better than that of PANI. Its initial specific capacitance values was 442 F g^{-1} at 5 mA cm^{-2}, and the value was approximate 100 F g^{-1} more than that of PANI. The energy density of T-PANI was higher at the range of same power density. The solution resistance, charge transfer resistance and diffuse resistance of T-PANI were also lower than these of PANI. The specific capacitance value remained about 30% of its initial capacitance after 2000 charge-discharge cycles. The high electrochemical performance of T-PANI was attributed to the improvements in specific surface area, pore structure, pore distribution and the ability to transfer electronic ascribing to PANI thorn grown on fibers surface. It signifies that modifying surface morphology of one-dimensional PANI can be a new idea for ideal supercapacitor electrode materials.

ACKNOWLEDGMENTS

This work was supported by the National Natural Science Foundation of China (No. 51203071 and 51363014), and Natural Science Funds of the Gansu Province (1208RJZA162 and 1308RJYA038).

REFERENCES

1. Winter, M.; Brodd, R. *J. Chem. Rev.* **2004**, *104*, 4245.
2. Sivaraman, P.; Kushwaha, R. K.; Shashidhara, K.; Hande, V. R.; Thakur, A. P.; Samui, A. B.; Khandpekar, M. M. *Electrochim. Acta* **2010**, *55*, 2451.
3. Sudeshna, C.; Yogesh, S.; Panikar, S. A.; Rajan, J.; Seeram, R.; Subodh, M.; Madhavi, S. *J. Appl. Polym. Sci.* **2012**, *12*, 1.
4. Shi, Y.; Pan, L. J.; Liu, B. R.; Wang, Y. Q.; Cui, Y.; Bao, Z. A.; Yu, G. H. *J. Mater. Chem. A* **2014**, *2*, 6086.
5. Sharma, R. K.; Rastogi, A. C.; Desu, S. B. *Electrochem. Commun.* **2008**, *10*, 268.
6. Lota, K.; Khomenko, V.; Frackowiak, E. *J. Phys. Chem. Solids* **2004**, *65*, 295.
7. Zhang, H. M.; Zhao, Q.; Zhou, S. P.; Liu, N. J.; Wang, X. H.; Li, J.; Wang, F. S. *J. Power Sources* **2011**, *196*, 10484.
8. Song, M. K.; Cheng, S.; Chen, H. Y.; Qin, W. T.; Nam, K. W.; Xu, S. C.; Yang, X. Q.; Bongiorno, A.; Lee, J.; Bai, J. M.; Tyson, T. A.; Cho, J.; Liu, M. L. *Nano Lett.* **2012**, *12*, 3483.
9. Zuo, S. X.; Liu, W. J.; Yao, C.; Li, X. Z.; Kong, Y.; Liu, X. H.; Mao, H. H.; Li, Y. R. *J. Chem. Eng.* **2013**, *228*, 1092.
10. Dhawale, D. S.; Vinu, A.; Lokhande, C. D. *Electrochim. Acta* **2011**, *56*, 9482.
11. Sun, Y. Y.; Guo, G. H.; Yang, B. H.; Tian, Y.; He, M. H.; Liu, Y. Q.; Zhao, G. Z. *Synth. Met.* **2011**, *161*, 2206.
12. Wang, K.; Wu, H. P.; Meng, Y. N.; Wei, Z. X. *Small* **2014**, *10*, 14.
13. Sun, W.; Chen, X. Y. *J. Power Sources* **2009**, *193*, 924.
14. Dhawale, D. S.; Dubal, D. P.; Jamadade, V. S.; Salunkhe, R. R.; Lokhande, C. D. *Synth. Met.* **2010**, *160*, 519.
15. Lü, X. M.; WU, Q. F.; Mi, H. Y.; Zhang, X. G. *Acta Phys. Chim. Sin.* **2007**, *23*, 820.
16. Tan, Y. T.; Ran, F.; Wang, L. R.; Kong, L. B.; Kang, L. *J Appl. Polym. Sci.* **2013**, *127*, 1544.
17. Wang, L. R.; Ran, F.; Tan, Y. T.; Zhao, L.; Kong, L. B.; Kang, L. *Chin. Chem. Lett.* **2011**, *22*, 964.
18. Stejskal, J.; Sapurina, I.; Trchova, M. *Prog. Polym. Sci.* **2010**, *35*, 1420.
19. Chiou, N. R.; Epstein, A. *J. Adv. Mater.* **2005**, *17*, 1679.
20. Liu, J. L.; Zhou, M. Q.; Fan, L. Z.; Li, P.; Qu, X. H. *Electrochim. Acta* **2010**, *55*, 5819.
21. Ho, V.; Zhou, C.; Kulinsky, L.; Madou, M. *J. Micromech. Microeng.* **2013**, *23*, 46.
22. Ma, G. F.; Mu, J. J.; Zhang, Z. G.; Sun, K. J.; Peng, H.; Lei, Z. Q. *Acta Phys. Chim. Sin.* **2013**, *29*, 2385.
23. Hung, P. J.; Chang, K. H.; Lee, Y. F.; Hua, C. C.; Lin, K. M. *Electrochim. Acta* **2010**, *55*, 6015.
24. Ghenaatian, H. R.; Mousavi, M. F.; Rahmanifar, M. S. *Synth. Met.* **2011**, *161*, 2017.
25. Liu, J. L.; Zhou, M. Q.; Fan, L. Z.; Li, P.; Qu, X. H. *Electrochim. Acta* **2010**, *55*, 5819.
26. Li, H. Q.; Luo, J. Y.; Zhou, X. F.; Yu, C. Z.; Xia, Y. Y. *J. Electrochem. Soc.* **2007**, *154*, A731.
27. Ghaemi, M.; Ataherian, F.; Zolfaghari, A.; Jafari, A. *Electrochim. Acta* **2008**, *53*, 4607.
28. Sen, P.; De, A. *Electrochim. Acta* **2010**, *55*, 4677.
29. Chen, Y. L.; Hu, Z. A.; Chang, Y. Q.; Wang, H. W.; Zhang, Z. Y.; Yang, Y. Y.; Wu, H. Y. *J. Phys. Chem. C* **2011**, *115*, 2563.
30. Zhu, Z. Z.; Wang, G. C.; Sun, M. Q.; Li, X. W.; Li, C. Z. *Electrochim. Acta* **2011**, *56*, 1366.
31. Mastragostino, M.; Arbizzani, C.; Soavi, F. *Solid State Ionics* **2002**, *148*, 493.